International Journal of Microwave and Wireless Technologies

cambridge.org/mrf

Pulse splitting technique for low sidelobe time-modulated antenna array synthesis with harmonic suppression

Tarek Sallam[1,2] and Ahmed M. Attiya[3]

[1]School of Computer Science and Technology, Shandong Xiehe University, Jinan, China; [2]Faculty of Engineering at Shoubra, Benha University, Cairo, Egypt and [3]Microwave Engineering Dept., Electronics Research Institute (ERI), Cairo, Egypt

Research Paper

Cite this article: Sallam T, Attiya AM (2024) Pulse splitting technique for low sidelobe time-modulated antenna array synthesis with harmonic suppression. *International Journal of Microwave and Wireless Technologies* **16**(7), 1155–1161. https://doi.org/10.1017/S1759078724000825

Received: 10 December 2023
Revised: 6 August 2024
Accepted: 12 August 2024

Keywords:
genetic algorithm; linear antenna array; pattern synthesis; pulse splitting; sideband level; sidelobe level; time modulation

Corresponding author: Tarek Sallam; Email: sallam_1982@yahoo.com

Abstract

In this paper, pulse splitting approach is proposed to simultaneously reduce the sidelobe level (SLL) of fundamental signal and maximum sideband levels (SBLs) of harmonic signals for time-modulated linear array (TMLA). This is achieved by controlling only the periodic switching time sequence of each element of the TMLA. In pulse splitting, the on–off switching sequence of each radiating element is characterized by multiple rectangular sub-pulses within the modulation period which increase the degrees of freedom in order to better synthesize the desired fundamental pattern with simultaneous suppression of harmonic or sideband radiation. A genetic algorithm is employed to optimize the switch-on and switch-off instants of each sub-pulse for each element for 16-element uniform amplitude, phase, and space linear antenna array. The simulation results reveal that the proposed method can achieve the desired patterns with very low SLL and SBLs compared with previous published results.

Introduction

The desired antenna array pattern with a specified sidelobe level (SLL) and a first null beamwidth (FNBW) can be achieved by controlling the three basic parameters: amplitude, phase, and spacing between radiating elements [1–5]. However, this requires a high dynamic range of parameters with the use of costly and complicated feed network of attenuators/amplifiers and phase shifters having high insertion loss. Moreover, the inter-element spacing cannot be controlled in real-time applications.

To avoid the aforementioned problems of conventional antenna arrays, "time modulation" is introduced [6, 7]. In time-modulated antenna arrays, "time" is considered as an additional dimension or degree of freedom to synthesize the radiation pattern simply by periodic on–off switching of array elements in a pre-defined sequence [8–10]. In this way, the radiation pattern at the fundamental frequency can be controlled to achieve low SLL with a small sacrifice in FNBW without the need of complex and expensive attenuators/amplifiers and phase shifters responsible for high insertion loss [11]. Moreover, time can be controlled electronically through radio-frequency (RF) switches which make it easier and more accurate to be implemented in real-time operation. Consequently, the proposed approach is a good candidate for achieving multiple goals such as SLL reduction and sideband level (SBL) suppression by utilizing solely time modulation.

However, due to the periodic switching of array elements, an infinite number of harmonics or sidebands is produced at multiples of time modulation frequency at either side of the carrier or fundamental frequency which is considered as waste of power reducing the radiation efficiency at the fundamental frequency and may interfere with other communication systems [12, 13]. Several evolutionary optimization algorithms have been adopted to minimize SBLs, and hence reducing sideband radiation such as genetic algorithm (GA) [14], differential evolution [15], particle swarm optimization [16], simulated annealing [17], and artificial bee colony [18]. These optimization algorithms have been extended to other approaches such as nonuniform element spacing [19], pulse shifting [20], and pulse splitting [21] to mitigate sideband radiation. In [22], improved harmony search algorithm is applied for simultaneous lowering of SLL of fundamental pattern and SBLs of sidebands. However, these methods, beside time modulation, employ other forms of modulation (weighting) such as amplitude and/or phase or spacing which is impractical as explained above.

In this paper, a simultaneous reduction of SLL of fundamental pattern and a suppression of SBLs for the harmonic patterns is obtained by solely using time modulation via pulse splitting. In pulse splitting, each element's on-pulse is divided into multiple sub-pulses. In pulse splitting, the on–off switching sequence of each radiating element is characterized by multiple rectangular

© The Author(s), 2024. Published by Cambridge University Press in association with The European Microwave Association.

sub-pulses within the modulation period which increase the degrees of freedom in order to better synthesize the desired fundamental pattern with simultaneous suppression of harmonic or sideband radiation. Thanks to pulse splitting, the harmonic power is spread over a larger number of frequencies. This improves sidebands suppression performance as a result [23–25].

In this paper, each element's on-pulse is composed of two sub-pulses within time modulation period with each has its own on and off switching instants. 16-element linear array is taken as an example. Thus, a total of 64 time variables should be optimized. GA is chosen to optimize these time variables for obtaining a fundamental pattern with specified SLL and FNBW and sideband patterns with specified SBL (the same as the specified SLL of fundamental pattern). These multiple objectives are taken care of using a certain mask with the specified SLL (or SBL) and FNBW. The time variables are optimized by minimizing the error between this mask and fundamental, first positive sideband, and second positive sideband patterns. The obtained results show that the SBLs of other sidebands are also suppressed although they are not taken into consideration in the optimization. To validate the effectiveness of the proposed approach, the numerical results are compared to other published results utilized different optimization algorithms. The proposed approach outperforms other previous approaches in terms of the achieved SLL and SBLs validating the effectiveness of the proposed approach.

Theory and problem formulation

Assume N-element time-modulated linear array (TMLA) consisting of uniform amplitude, phase, and spacing isotropic elements placed along the positive z-axis, and controlled via RF switches. In this case, the array factor of TMLA is defined as

$$AF(\theta, t) = e^{j2\pi f_0 t} \sum_{n=1}^{N} U_n(t)\, e^{j\beta(n-1)d\cos\theta} \tag{1}$$

where $\beta = 2\pi/\lambda$ is the propagation constant with λ being the wavelength at the fundamental frequency f_0, and d is the uniform spacing between array elements. The switching modulation function of nth element is given by $U_n(t)$, $n = 1, 2, \ldots, N$. θ is the elevation angle of the array.

Since the modulation function is periodic with time modulation frequency f_p ($f_p \ll f_0$), it can be expressed by Fourier series, given by

$$U_n(t) = \sum_{m=-\infty}^{\infty} a_{mn} e^{j2\pi m f_p t} \tag{2}$$

where a_{mn} is the complex Fourier coefficient of nth element at m harmonic mode ($m = 0, \pm1, \pm2, \ldots, \pm\infty$) with $m = 0$ represents array fundamental frequency, while the rest values of m represent the harmonic frequencies emerged as a result of time modulation. a_{mn} is given by

$$a_{mn} = \frac{1}{T_p} \int_0^{T_p} U_n(t) e^{-j2\pi m f_p t} dt \tag{3}$$

where T_p is the time modulation period, $T_p = 1/f_p$. Now, the array factor of TMLA can be expressed as

$$AF(\theta, t) = \sum_{m=-\infty}^{\infty} \sum_{n=1}^{N} a_{mn} e^{j\beta(n-1)d\cos\theta} e^{j2\pi(f_0 + m f_p)t} \tag{4}$$

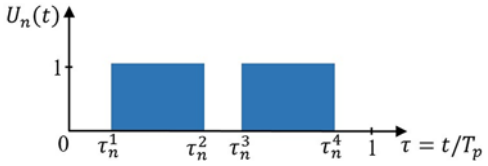


Figure. 1. The switching scheme of pule-split.

The array factor for mth order harmonic frequency can be further simplified as

$$AF_m(\theta, t) = e^{j2\pi(f_0 + m f_p)t} \sum_{n=1}^{N} a_{mn} e^{j\beta(n-1)d\cos\theta} \tag{5}$$

where harmonic radiation patterns occur at $m = \pm1, \pm2, \ldots, \pm\infty$, while the fundamental radiation pattern occurs at $m = 0$. In this study, the by-product harmonics represent power loss in unintended directions that should be suppressed as possible.

Pulse splitting

The switching scheme of pulse-split is shown in Fig. 1. The y-axis represents the switching modulation function for nth element $U_n(t)$, while the x-axis represents time normalized to modulation period $\tau = t/T_p$. The on-time pulse for nth element is divided into two on-time sub-pulses with off state between them. The first sub-pulse has switching on and off instants τ_n^1 and τ_n^2, respectively. The switching on and off instants of second sub-pulse are τ_n^3 and τ_n^4, respectively. There is an off state between τ_n^2 and τ_n^3, i.e., $\tau_n^3 - \tau_n^2 = 0$. The modulation function for pulse-split within modulation period (i.e.,$\tau_n^1 < \tau_n^2 < \tau_n^3 < \tau_n^4 < 1$) is expressed by

$$U_n(t) = \begin{cases} 1, & \tau_n^1 < \tau < \tau_n^2 \\ 1, & \tau_n^3 < \tau < \tau_n^4 \\ 0, & otherwise \end{cases} \tag{6}$$

The corresponding Fourier coefficient can be derived as

$$a_{mn} = (\tau_n^2 - \tau_n^1)\mathrm{sinc}\left(m\pi(\tau_n^2 - \tau_n^1)\right)e^{-jm\pi(\tau_n^1 + \tau_n^2)} + (\tau_n^4 - \tau_n^3)\mathrm{sinc}\left(m\pi(\tau_n^4 - \tau_n^3)\right)e^{-jm\pi(\tau_n^3 + \tau_n^4)} \tag{7}$$

Cost function

First of all, a mask is defined with a specified SLL which is the desired SLL (or SBL). Also, the mask has a specified FNBW which is the desired FNBW of fundamental pattern. To achieve the desired fundamental pattern with a simultaneous suppression of sideband patterns, the switching on/off instants of all sub-pulses for all elements should be determined through an optimization (minimization) of a properly defined cost function that covers the design specifications. The cost function is considered as the total error between mask and fundamental pattern along with first two positive sideband patterns. Thus, the total error consists of three components. The first component ε_0 is the error between the array factor of fundamental pattern AF_0 and *mask*, given by

https://doi.org/10.1017/S1759078724000825 Published online by Cambridge University Press

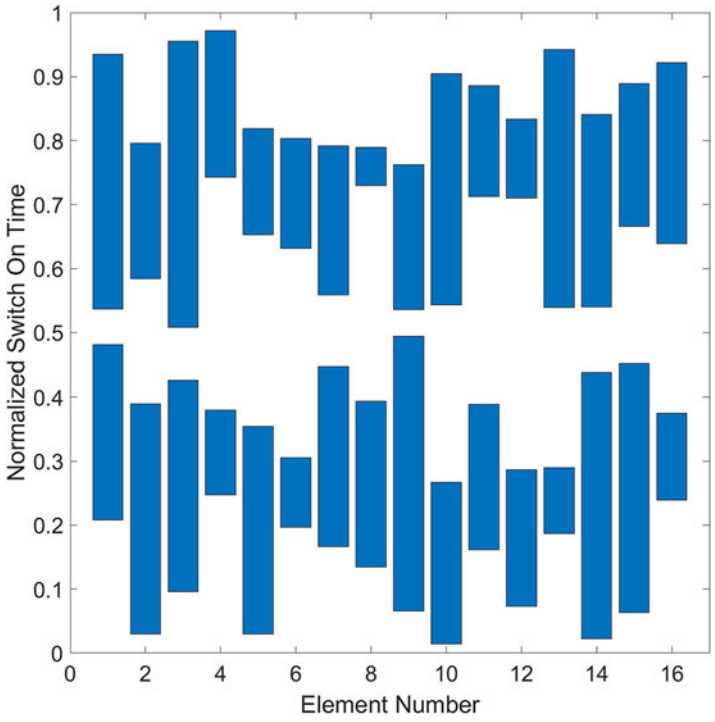


Figure 2. Initial switching sequence for 16-element TMLA.

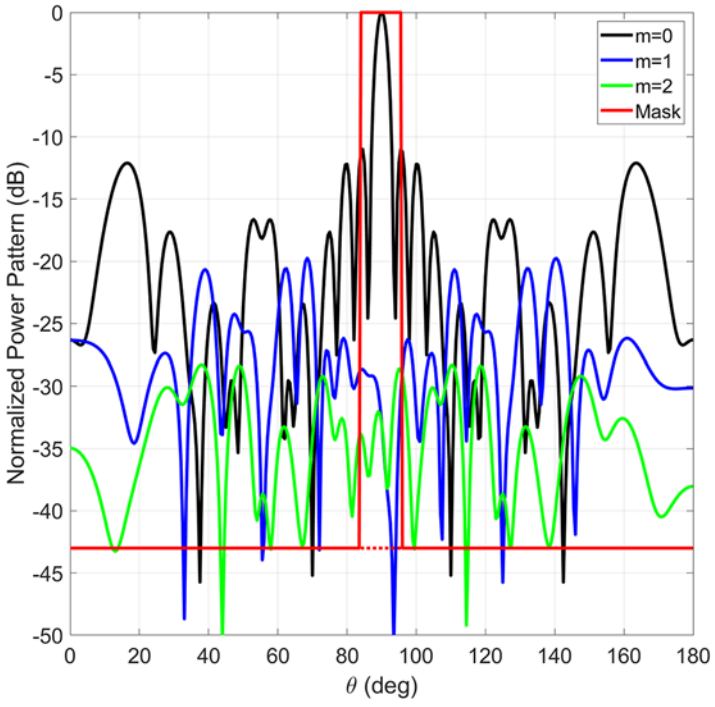


Figure 3. Initial radiation patterns for 16-elelemt TMLA.

$$\varepsilon_0(\theta) = \frac{1 + \mathrm{sgn}\left(AF_0(\theta) - mask(\theta)\right)}{2}\left[AF_0(\theta) - mask(\theta)\right] \quad (8)$$

The sign function sgn(θ) indicates that the error is expressed by "don't exceed" criterion meaning that only the pattern points of array factor those are greater than the mask contribute to the score of the error. Note that this error is computed at a certain combination of switching on and off instants of sub-pulses, so the time variable is dropped from array factor. The second and third components ε_1 and ε_2 are defined as the "don't exceed" errors between SLL of mask SLL_{mask} and array factors of 1st and 2nd positive sidebands AF_1 and AF_2, respectively, defined as

$$\varepsilon_{1,2}(\theta) = \frac{1 + \mathrm{sgn}\left(AF_{1,2}(\theta) - SLL_{mask}\right)}{2}\left[AF_{1,2}(\theta) - SLL_{mask}\right] \quad (9)$$

The total error thus given by

$$\varepsilon(\theta) = w_0 * \varepsilon_0(\theta) + w_1 * \varepsilon_1(\theta) + w_2 * \varepsilon_2(\theta) \quad (10)$$

https://doi.org/10.1017/S1759078724000825 Published online by Cambridge University Press

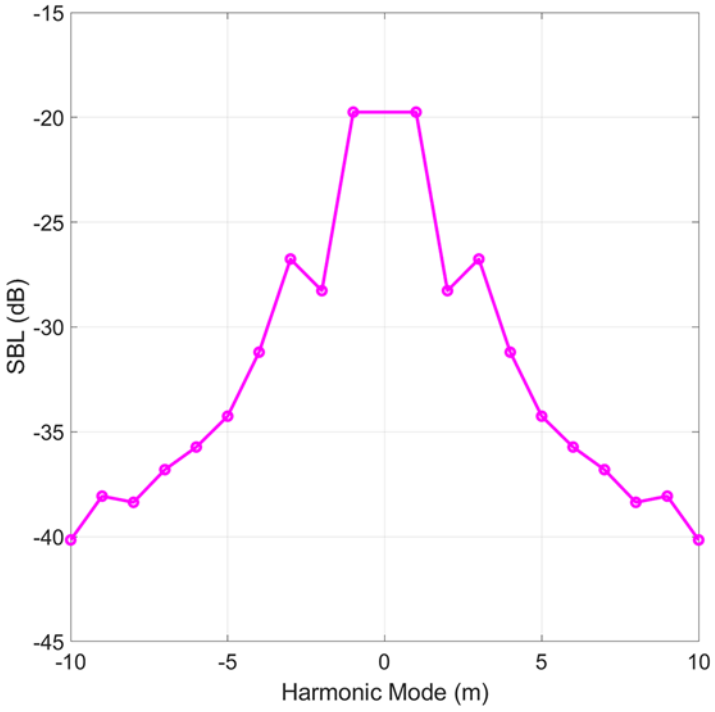


Figure 4. Initial SBLs for 16-elemnt TMLA for $|m| \leq 10$.

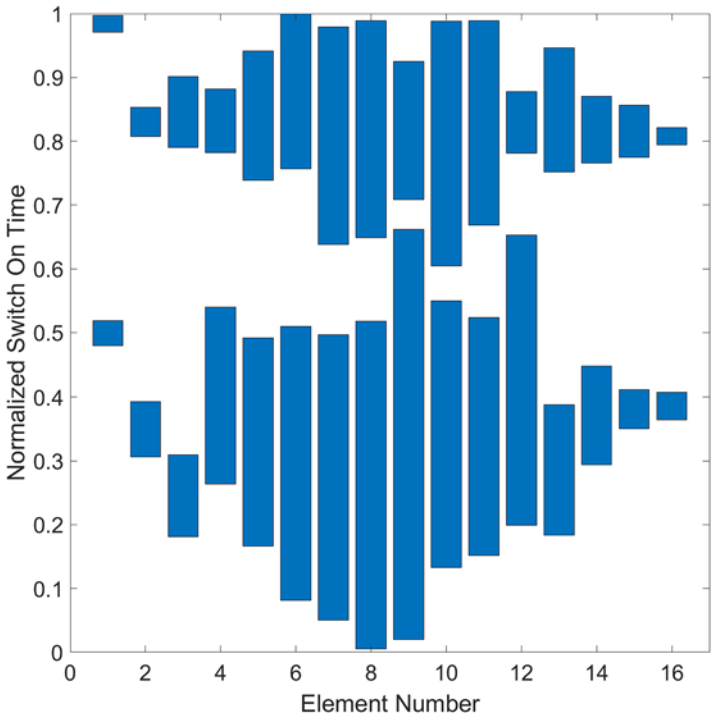


Figure 5. Optimized switching sequence for 16-element TMLA.

where w_0, w_1, and w_2 are weighting factors for the three components of the total error. The cost function is the total error averaged over all samples of the elevation angle Θ

$$CF = \frac{1}{\Theta} \sum_{i=1}^{\Theta} \varepsilon(\theta_i) \tag{11}$$

GA is employed to minimize the cost function to get the optimum switching on and off instants with each chromosome (individual) of the population has a dimension of 4 N which is the same as the dimension of the optimization problem (the total number of switching on and off instants). Detailed discussions on GA can be found in [26–29], and its applications to antenna array synthesis are reported in [1, 2, 30–33].

https://doi.org/10.1017/S1759078724000825 Published online by Cambridge University Press

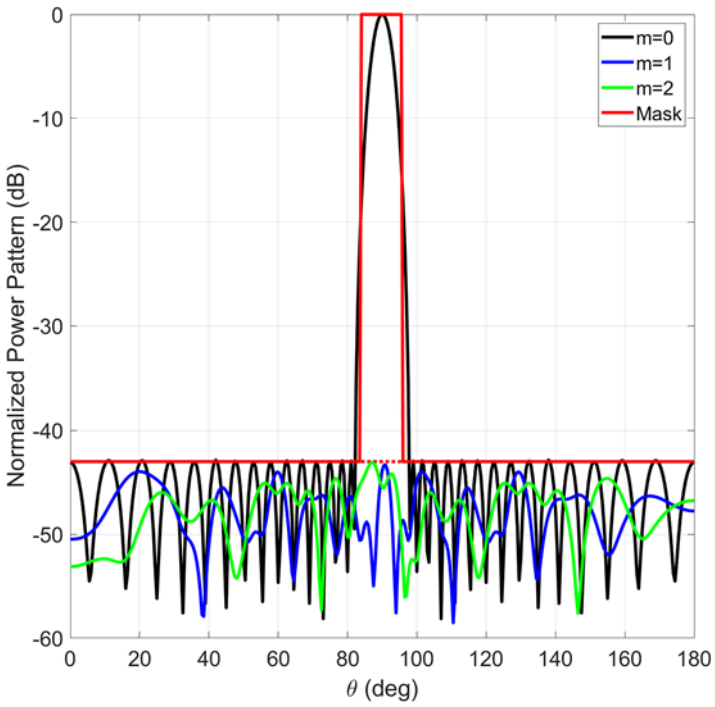


Figure 6. Optimized radiation patterns for 16-element TMLA.

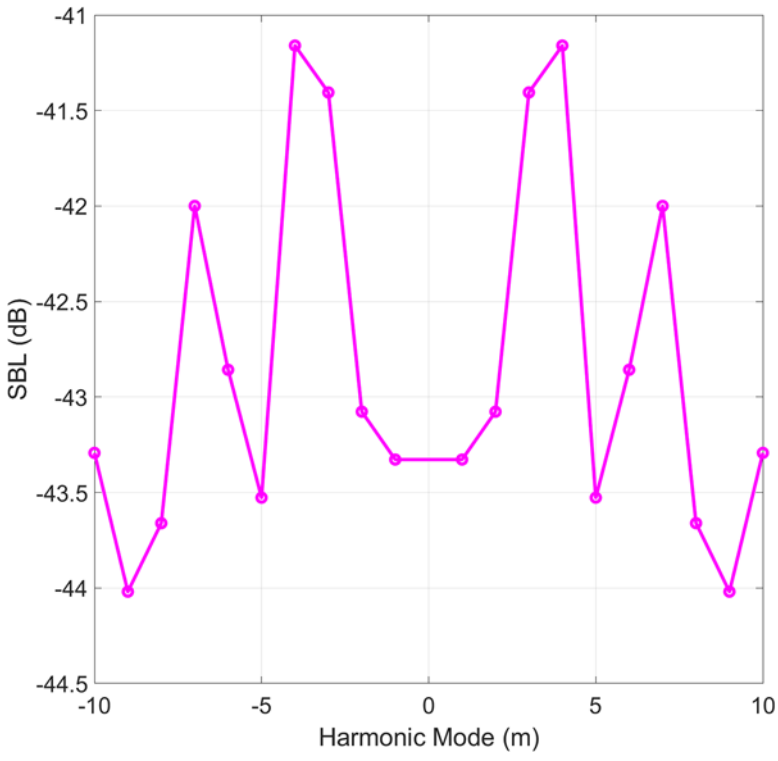


Figure 7. Optimized SBLs for 16-elemnt TMLA for $|m| \leq 10$.

Results and discussion

Consider 16-element uniform amplitude, phase, and spacing TMLA. In this case, we have a total of 64 switching on and off instants to be optimized. After many simulation trials, the inter-element spacing d is chosen as 0.88λ which leads to better results than the usual spacing $\lambda/2$ The fundamental frequency f_0 is 10 GHz and time modulation frequency $f_p = 1$ MHz. All numerical results are obtained with the aid of MATLAB R2023a. The GA is also implemented in MATLAB using the "ga" function with a population size of 200. The optimization is terminated when average change in value of the cost function is less than 0.01.

https://doi.org/10.1017/S1759078724000825 Published online by Cambridge University Press

Table 1. Comparison of optimized SLL and $SBL_{1,2}$ between proposed approach and other approaches

Approach	SLL (dB)	SBL_1 (dB)	SBL_2 (dB)
[14]	−25.50	−24.60	–
[20]	−30.00	−19.50	−21.70
[21]	−30.00	−22.51	–
[24]	−30.00	−27.80	–
[35] (Ex#1)	−30.00	−20.21	−22.33
[35] (Ex#2)	−30.00	−19.28	−20.79
[36]	−30.00	−21.12	–
[22]	−40.31	−29.47	−32.59
Proposed	**−42.84**	**−43.33**	**−43.08**

The optimization starts with an initial set of all variables (switching on and off instants) defined randomly within the normalized modulation period (from 0 to 1), and also constrained within this period during optimization process. Figure 2 shows the initial (before optimization) switching sequence for all array elements.

Figure 3 shows the mask along with initial fundamental ($m = 0$) and first two positive ($m = 1, 2$) sideband patterns. After several trials, the SLL of mask SLL_{mask} is chosen to be −43 dB, as shown in Fig. 3, which represents the desired SLL of fundamental pattern or desired maximum SBL of sideband patterns. This mask's SLL is chosen such that it is the lowest level the SLL of fundamental pattern can reach with an acceptable error. The FNBW of mask (the desired FNBW of fundamental pattern) is 12.

As shown in Fig. 3, the initial FNBW of fundamental pattern is 8°. The initial SLL of fundamental pattern *SLL*, SBL of 1st sideband SBL_1, and SBL of 2nd sideband SBL_2 are −10.99 dB, −19.75 dB, and −28.27 dB, respectively. As can be noticed, SBL_2 is the lowest level among the three levels. Thus, it is expected that 2nd sideband pattern will be easier to be optimized than the fundamental and 1st sideband patterns. That is why the weighting factor for 2nd sideband w_2 should be chosen to be less than the other weighting factors of cost function w_0 and w_1. After several runs, the three factors are selected as $w_0 = 1$, $w_1 = 1$, and $w_2 = 0.25$. In this case, the initial value of cost function is 35.41 dB. Figure 4 shows the initial SBLs for first positive and negative ten harmonics. As can be shown, all initial SBLs are under the level of 1st sideband which is −19.75 dB and also above a level of about −40 dB.

Figure 5 shows the optimized (after optimization) switching sequence for 16-element TMLA. As can be shown, the total on-time duration decreases from center to outer elements with center elements have the longest total on-time duration, while the outer elements have the shortest ones. This ensures a high feeding network efficiency [34]. Figure 6 shows the optimized radiation patterns for fundamental and first two sideband frequencies along with mask. It is can be noticed that *SLL*, SBL_1, and SBL_2 are well suppressed under SLL_{mask}. The optimized *SLL*, SBL_1, and SBL_2 are −42.84 dB, −43.33 dB, and −43.08 dB, respectively. The optimized FNBW of fundamental pattern is 16° exceeding the desired FNBW by 4° which is a little sacrifice compared to the high gain in reducing SLL of fundamental pattern. The final value of cost function after optimization is 0.32 dB.

Fig. 7 shows the optimized SBLs for first positive and negative ten harmonics. As can be shown, all SBLs after optimization become under a level of −41 dB. The higher-order SBLs are also well suppressed, although they are not included in the formulation of cost function that was optimized.

To highlight the efficacy of the proposed approach, the optimized results for *SLL* and $SBL_{1,2}$ are compared with other published approaches for 16-element TMLA and presented in Table 1. The proposed approach outperforms other approaches in terms of SLL and SBLs. The optimized SLL of the fundamental pattern is lowered to −42.84 dB compared to the best result of −40.31 dB [22]. The first and second positive SBLs are considerably improved to −43.33 and −43.08 dB from the best results of −29.47 and −32.59 dB [22], respectively.

Conclusion

In this paper, a simultaneous reduction of SLL of fundamental pattern and suppression of SBLs of generated harmonics of TMLAs is presented with optimized switching sequences. A pulse splitting technique is employed to give more degrees of freedom to simultaneously realize the desired radiation patterns in a GA-based approach. This is achieved by controlling only the periodic pulse-split sequences, which also eliminates the need for attenuators and/or phase shifters. The proposed approach outperforms other previous approaches in terms of the achieved SLL and SBLs validating the effectiveness of the proposed approach. The proposed method also maintains a narrow FNBW, which implies a highly directive main beam at the fundamental pattern. Consequently, the proposed approach is promising for achieving multiple goals such as SLL reduction, SBL suppression, and directivity maximization all by utilizing merely time modulation.

Competing interests. The authors declare none.

References

1. **Sallam T and Attiya AM** (2019) Different array synthesis techniques for planar antenna array. *Applied Computational Electromagnetics Society Journal* **34**, 716–723.
2. **Sallam T and Attiya A** (2020) Low sidelobe cosecant-squared pattern synthesis for large planar array using genetic algorithm. *Progress In Electromagnetics Research M* **93**, 23–34.
3. **Sallam T and Attiya A** (2020) Low sidelobe wide nulling digital beamforming for large planar array using iterative FFT techniques. *Progress In Electromagnetics Research M* **90**, 37–46.
4. **Sallam T and Attiya A** (2017) Sidelobe reduction and resolution enhancement by random perturbations in periodic antenna arrays. *The 34th National Radio Science Conference (NRSC'17)*, Alexandria, Egypt, 49–55.
5. **Elliott RS** (2003) *Antenna Theory and Design*, Revised edition. New Jersey: IEEE Press.
6. **Shanks HE and Bickmore RW** (1959) Four-dimensional electromagnetic radiators. *Canadian Journal of Physics* **37**, 263–275.
7. **Haupt RL** (2017) Antenna arrays in the time domain: An introduction to timed arrays. *IEEE Antennas and Propagation Magazine* **59**, 33–41.
8. **Varma DS, Ram G and Kumar GA** (2023) Time-modulated arrays: A review. *IETE Technical Review* **40**, 136–151.
9. **Maneiro-Catoira R, Brégains J, García-Naya JA and Castedo L** (2017) Time modulated arrays: From their origin to their utilization in wireless communication systems. *Sensors* **17**, 590.
10. **Rocca P, Yang F, Poli L and Yang S** (2019) Time-modulated array antennas – Theory, techniques, and applications. *Journal of Electromagnetic Waves and Applications* **33**, 1503–1531.
11. **Kummer W, Villeneuve A, Fong T and Terrio F** (1963) Ultra-low sidelobes from time-modulated arrays. *IEEE Transactions on Antennas and Propagation* **11**, 633–639.

https://doi.org/10.1017/S1759078724000825 Published online by Cambridge University Press

12. **Bregains JC, Fondevila-Gomez J, Franceschetti G and Ares F** (2008) Signal radiation and power losses of time-modulated arrays. *IEEE Transactions on Antennas and Propagation* **56**, 1799–1804.
13. **Yang S, Gan YB and Tan PK** (2004) Evaluation of directivity and gain for time-modulated linear antenna arrays. *Microwave and Optical Technology Letters* **42**, 167–171.
14. **Yang S, Gan YE, Qing A and Tan PK** (2005) Design of a uniform amplitude time modulated linear array with optimized time sequences. *IEEE Transactions on Antennas and Propagation* **53**, 2337–2339.
15. **Yang S, Gan YB and Qing A** (2002) Sideband suppression in time-modulated linear arrays by the differential evolution algorithm. *IEEE Antennas and Wireless Propagation Letters* **1**, 173–175.
16. **Poli L, Rocca P, Manica L and Massa A** (2010) Handling sideband radiations in time-modulated arrays through particle swarm optimization. *IEEE Transactions on Antennas and Propagation* **58**, 1408–1411.
17. **Fondevila J, Bregains JC, Ares F and Moreno E** (2006) Application of time modulation in the synthesis of sum and difference patterns by using linear arrays. *Microwave and Optical Technology Letters* **48**, 829–832.
18. **Nakanishi T, Kihira K, Takahashi T, Konishi Y and Chiba I** (2013) Sideband suppression using switched phase distribution in time-modulated array antennas. *2013 IEEE International Symposium on phased array systems and technology*, 521–528.
19. **Li G, Yang S, Huang M and Nie Z** (2010) Sidelobe suppression in time modulated linear arrays with unequal element spacing. *Journal of Electromagnetic Waves and Applications* **24**, 775–783.
20. **Poli L, Rocca P, Manica L and Massa A** (2010) Pattern synthesis in time-modulated linear arrays through pulse shifting. *IET Microwaves, Antennas & Propagation* **4**, 1157–1164.
21. **Aksoy E and Afacan E** (2011) Sideband level suppression improvement via splitting pulses in time modulated arrays under static fundamental radiation. *PIERS Proceedings*, Suzhou, China, 364–367.
22. **Chakraborty A, Ram G and Mandal D** (2020) Optimal pulse shifting in timed antenna array for simultaneous reduction of sidelobe and sideband level. *IEEE Access* **8**, 131063–131075.
23. **Yang S, Gan YE, Qing A and Tan PK** (2005) Design of a uniform amplitude time modulated linear array with optimized time sequences. *IEEE Transactions on Antennas and Propagation* **53**, 2337–2339.
24. **Zhu Q, Yang S, Zheng L and Nie Z** (2012) Design of a low sidelobe time modulated linear array with uniform amplitude and sub-sectional optimized time steps. *IEEE Transactions on Antennas and Propagation* **60**, 4436–4439.
25. **Tong Y and Tennant A** (2012) Sideband level suppression in time-modulated linear arrays using modified switching sequences and fixed bandwidth elements. *IET Electronics Letters* **48**, 10–11.
26. **Holland JH** (1992) Genetic algorithms. *Scientific American* **267**, 66–72
27. **Goldberg DE** (1989) *Genetic Algorithms in Search, Optimization, and Machine Learning*. MA: Addison-Wesley.
28. **Haupt RL and Haupt SE** (2004) *Practical Genetic Algorithms*, 2nd edition. New York: John Wiley & Sons.
29. **Haupt RL and Werner D** (2007) *Genetic Algorithms in Electromagnetics*. New York: John Wiley & Sons.
30. **You P, Liu Y, Xu KD, Zhu C and Liu QH** (2017) Generalisation of genetic algorithm and fast Fourier transform for synthesising unequally spaced linear array shaped pattern including coupling effects. *IET Microwaves, Antennas & Propagation* **11**, 827–832.
31. **Boeringer DW and Werner DH** (2004) Particle swarm optimization versus genetic algorithms for phased array synthesis. *IEEE Transactions on Antennas and Propagation* **52**, 771–779.
32. **Ibarra M, Panduro MA, Andrade ÁG and Reyna A** (2015) Design of sparse concentric rings array for LEO satellites. *Journal of Electromagnetic Waves and Applications* **29**, 1983–2001.
33. **Reyna A, Panduro MA, Covarrubias DH and Mendez A** (2012) Design of steerable concentric rings array for low side lobe level. *Scientia Iranica* **19**, 727–732.
34. **Zhu Q, Yang S, Yao R and Nie Z** (2012) Gain improvement in time-modulated linear arrays using SPDT switches. *IEEE Antennas and Wireless Propagation Letters* **11**, 994–997.
35. **Yang J, Li W and Shi X** (2014) Phase modulation technique for four-dimensional arrays. *IEEE Antennas and Wireless Propagation Letters* **13**, 1393–1396.
36. **Ni G, He C, Chen J, Liu Y and Jin R** (2020) Low sideband radiation beam scanning at carrier frequency for time-modulated array by non-uniform period modulation. *IEEE Transactions on Antennas and Propagation* **68**, 3695–3704.



Tarek Sallam was born in Cairo, Egypt, in 1982. He received the B.S. degree in electronics and telecommunications engineering and the M.S. degree in engineering mathematics from Benha University, Cairo, Egypt, in 2004 and 2011, respectively, and the Ph.D. degree in electronics and communications engineering from Egypt-Japan University of Science and Technology, Alexandria, Egypt, in 2015. In 2006, he joined the Faculty of Engineering at Shoubra, Benha University. In 2019, he joined Huaiyin Institute of Technology, Huai'an, China. In 2022, he joined Qujing Normal University, Qujing, China. In 2024, he joined the School of Computer Science and Technology, Shandong Xiehe University, Jinan, China, where he is currently an Associate Professor. He was a Visiting Researcher with the Electromagnetic Compatibility Lab, Osaka University, Osaka, Japan. His research interests include evolutionary optimization, neural networks and deep learning, phased array antennas with array signal processing and adaptive beamforming.



Ahmed M. Attiya M.Sc. and Ph.D. Electronics and Electrical Communications, Faculty of Engineering, Cairo University at 1996 and 2001 respectively. He joined Electronics Research Institute as a Researcher Assistant in 1991. In the period from 2002 to 2004 he was a Postdoc in Bradley Department of Electrical and Computer Engineering at Virginia Tech. In the period from 2004 to 2005 he was a Visiting Scholar in Electrical Engineering Dept. in University of Mississippi. In the period from 2008 to 2012 he was a Visiting Teaching Member in King Saud University. He is currently Full Professor and the Head of Microwave Engineering Dept. in Electronics Research Institute. He is also the Founder of Nanotechnology Lab. in Electronics Research Institute.

https://doi.org/10.1017/S1759078724000825 Published online by Cambridge University Press